4-P-202

# Evaluation of interfacial OH radical transport using plasma exposed high-speed water jet

K. Takeda , S. Sasaki, K. Takashima and T. Kaneko

*Graduate School of Engineering, Tohoku University, Sendai, Japan*

**Abstract:** Interfacial transport of reactive spicies such as OH radical ($^{\bullet}$OH) is an important topic for applications using atmospheric pressure plasmas (APPs), but are hardly characterized experimentally and not fully revealed. In this study using an APP system with a high-speed water jet, very fast decay (a half-life of ~ 0.1 ms) of $^{\bullet}$OH was detected and explained with a numerical model assuming surface-localization of $^{\bullet}$OH. The consistency between the experiment and the calculation led us the influx of interfacial $^{\bullet}$OH as the $4.5\times 10^{19}$ m$^{-2}$ s$^{-1}$.

**Keywords:** Plasma-liquid interaction , OH radical, Atmospheric pressure plasma

## 1. Introductioin

Novel applications of non-equilibrium atmospheric pressure plasmas (APPs) in contact with a liquid are studied extensively. These applications employ APP as a source to deliver the reactive oxygen and nitrogen species (RONS) to the liquid phase, while much of the RONS chemistry at the plasma-liquid interface is not fully understood. Notably, distributions of short-lived RONS (*e.g.*, $^{\bullet}$OH, $HO_2$, NO) are hardly characterized due to their high reactivity and nonuniformity. Because the predominant reactions by APP can occur near the interface, experimental characterization on the spatial and temporal distribution of short-lived RONS can be critical discussion in the reactive species chemistry at the interface.

Recently, P. Rumbach *et al*,. built a simple reaction-diffusion model of $^{\bullet}$OH [1]. Their model described the localized $^{\bullet}$OH distribution as a function of its influx and co-dissolved species concentration. But this model assumes a self-similarity distribution valid if the $^{\bullet}$OH consumption by the uniformly distributed other reactive species is dominant. Thus, experimental detection and characterization method of liquid-phase $^{\bullet}$OH are still challenging.

In this study, we developed an APP system with high-speed water flow through APP. This system allows us to detect the experimental decay of $^{\bullet}$OH [2]. Furthermore, we built a numerical model based on a reaction-diffusion equation including chemical reactions with some stable RONS to understand the $^{\bullet}$OH behavior at the plasma-liquid interface.

## 2. Experimental setup

The experimental schematic is shown in Fig. 1. He-APP is generated by applying a high AC voltage ($V_{\mathrm{p\text{-}p}}$ = 8.8 kV, $f \approx$ 9 kHz) to the copper foil which is attached on the outside of the quartz tube. Distilled water flow at approximately $F_{DW}$ = 10 mL/min is jetted at a speed of 12.6 m/s from a grounded stainless tube with inner diameter of 0.13 mm, which is set in the upstream region on the central axis. At the downstream region, the Teflon plate on the grounded electrode with a hole (φ = 0.8 mm) is set to shut out the plasma plume propagation. To detect the cross sectional average concentration of $^{\bullet}$OH ([$^{\bullet}$OH]$_{\mathrm{csa}}$), terephthalic acid (TA) reagent which reacts with $^{\bullet}$OH to form the 2-hydroxylterephthalate ion (HTA$^{2-}$) as a highly fluorescent material was used as the reagent flow. The reagent flow at approximately 1.1 mL/min is jetted from a PEEK tube with inner diameter of 0.11 mm to water flow. This mixing position is accurately controlled at least 1 mm by the Z-stage. The high-speed water flow provides a spatial resolution of 1 mm, corresponding to the time resolution of approximately 0.08 ms. Thus, we can accurately control the distance from the plasma plume end to the reagent flow injection port ($d_{\mathrm{g}}$) and measure the $^{\bullet}$OH decay with high temporal resolution.

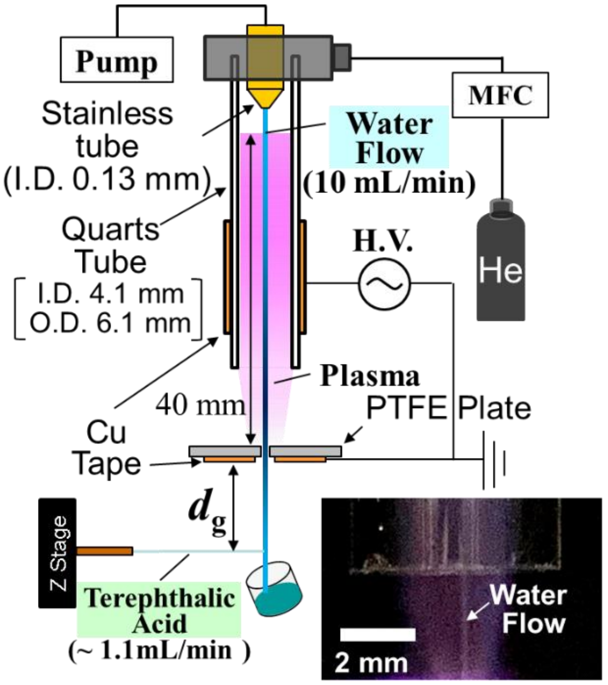

Fig. 1 Schematic drawing of the APP system with high-speed water jet.

## 3. Numerical modelling of $^{\bullet}$OH

In order to explain the experimental rapid decay of liquid-phase $^{\bullet}$OH , we built two types of the numerical model. Figure 2 shows the (A) homogeneous model and (B) suface-localized distribution of $^{\bullet}$OH. In both models, $^{\bullet}$OH is consumed by co-dissolved RONS based on the following reactions [3].

$$^{\bullet}\mathrm{OH} + {}^{\bullet}\mathrm{OH} \rightarrow \mathrm{H_2O_2}\ (k_{\mathrm{OH}} = 4.2 \times 10^{9}\ \mathrm{M^{-1}s^{-1}})$$
$$^{\bullet}\mathrm{OH} + \mathrm{H_2O_2} \rightarrow \mathrm{HO_2} + \mathrm{H_2O}\ (k_{\mathrm{H2O2}} = 2.7 \times 10^{7}\ \mathrm{M^{-1}s^{-1}})$$
$$^{\bullet}\mathrm{OH} + \mathrm{NO_2}^{-} \rightarrow \mathrm{OH}^{-} + \mathrm{NO_2}\ (k_{\mathrm{NO2-}} = 6.0 \times 10^{9}\ \mathrm{M^{-1}s^{-1}})$$

Here, 6.5 μM $H_2O_2$ and 0.5 μM $NO_2^-$ were experimentally measured at the collected water flow passing through the APP, and these values were used in the calculation. The rate of the second-order reaction of $^{\bullet}$OH strongly depends on the $^{\bullet}$OH concentration. In the surface localized model (B), the $^{\bullet}$OH decay is significantly changed by the $^{\bullet}$OH distribution even if having same $[^{\bullet}\mathrm{OH}]_{\mathrm{csa}}$ values. In addition, the diffusion of $^{\bullet}$OH should be simultaneously considered with the chemical consumption of $^{\bullet}$OH. Then, the following reaction-diffusion equation is used in the model (B).

$$\frac{\partial[^{\bullet}\mathrm{OH}]}{\partial t} - D_{\mathrm{OH}}\frac{d^2[^{\bullet}\mathrm{OH}]}{dx^2} = f([^{\bullet}\mathrm{OH}])$$

where, $D_{\mathrm{OH}} = 2.3 \times 10^{-9}\ \mathrm{m^2\ s^{-1}}$ is the room temperature diffusivity of $^{\bullet}$OH obtained from the literature [1]. $f([^{\bullet}\mathrm{OH}])$ is the reaction term by the three chemical reactions mentioned above. To solve this reaction-diffusion equation, boundary conditions are given at a plasma-liquid interface and 10 μm depth (where $[^{\bullet}\mathrm{OH}]$ is assumed to be almost zero). At a plasma-liquid interface, the influx of $^{\bullet}$OH ($\Gamma_{\mathrm{OH}}$) was given in the form of $d[^{\bullet}\mathrm{OH}]/dx$ as a Neumann condition. At 10 μm depth, the $^{\bullet}$OH gradient was assumed to be 0.

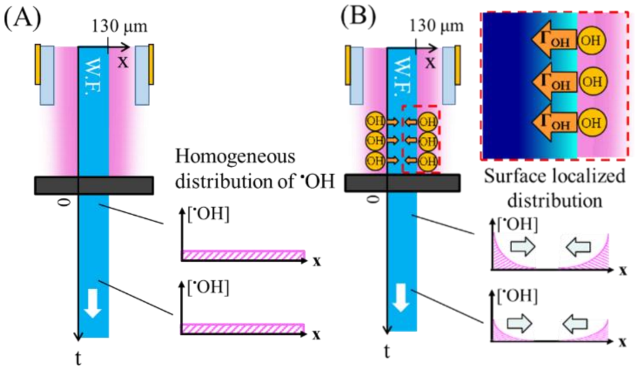

Fig. 2 The simulation models assuming (A) homogeneous and (B) surface localized distribution of $^{\bullet}$OH.

## 4. Results and discussion

Figure 3 shows the experimental plots of $[^{\bullet}\mathrm{OH}]_{\mathrm{csa}}$ decay and calculation results with (A) a homogeneous distribution model and (B) a highly surface localized model. Here, details of $[^{\bullet}\mathrm{OH}]_{\mathrm{csa}}$ quantification can be found in [2]. As shown in black plots in Fig. 3, the experimental $[^{\bullet}\mathrm{OH}]_{\mathrm{csa}}$ immediately after plasma exposure was 88 nM, and the half-life was approximately 0.1 ms. In the model (A), the simulation result was discrepant with the experimental $[^{\bullet}\mathrm{OH}]_{\mathrm{csa}}$ decay. This discrepancy can be due to the oversimplification of the $^{\bullet}$OH distribution because the rate of the second-order reaction with $^{\bullet}$OH strongly depend on the $^{\bullet}$OH concentration inside the water flow. On the other hand, the calculation based on model (B) was in good agreement with the experimental $[^{\bullet}\mathrm{OH}]_{\mathrm{csa}}$ decay. Then, the $[^{\bullet}\mathrm{OH}]$ transfer flux from plasma into the liquid surface $\Gamma_{\mathrm{OH}} = 4.5 \times 10^{19}\ \mathrm{m^{-2}s^{-1}}$ can be found from the fitting in Fig. 3. In addition, the surface localized modeling with the experimental results can potentially characterize not only $\Gamma_{\mathrm{OH}}$ but also the temporal and spatial distribution of the liquid phase $^{\bullet}$OH. The characteristics penetration depth of $^{\bullet}$OH defined as a depth at which the $[^{\bullet}\mathrm{OH}]|_{t=0}$ falls to 1/e is approximately 300 nm, from the consistency of the experimental decay and the numerical calculations. This penetration depth is also discussed by the reported previous diffusion model [1].

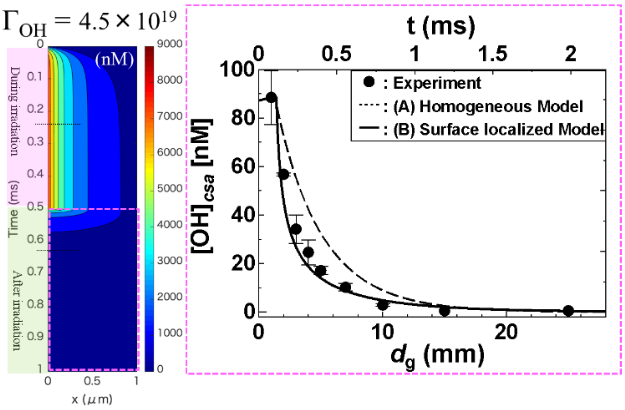

**Fig. 3.** The experimental plots of $[^{\bullet}\mathrm{OH}]_{\mathrm{csa}}$ and calculation results with (A) homogeneous and (B) highly surface localized models.

## Acnownledgmenet

This work was supported by JSPS KAKENHI (Grant Nos. 18H03687, 19K14698, 20H01890, and 22H04947), WISE Program for AI Electronics, cLPS Nagoya University, and RIEC Tohoku University.

## References

[1] P. Rumbach et al,. Plasma Sources Sci. Technol. **27**, 115013 (2018).
[2] K. Takeda et al., Appl. Phys. Express **14**, 056001 (2021).
[3] W. Tian and M. J. Kushner, J. Phys. D. Appl. Phys. 47, 165201 (2014).